Available online at www.sciencedirect.com
SCIENCE DIRECT®
International Journal of Heat and Mass Transfer 47 (2004) 787–795
International Journal of HEAT and MASS TRANSFER
www.elsevier.com/locate/ijhmt

The limits of the analogy between boiling and gas evolution at electrodes

H. Vogt *, Ö. Aras, R.J. Balzer

TFH Berlin, University of Applied Sciences, D-13353 Berlin, Germany

Received 7 March 2003; received in revised form 10 June 2003

Abstract

The processes of gas evolution at electrodes in electrochemical reactors and of boiling belong to strongly different fields in chemical engineering and for a long time were investigated separately. Nonetheless, they exhibit numerous common features. The analogies of both processes have been made use of giving rise to transfer findings obtained in one field to the other one. However, the analogy is limited, and the limitations have not yet attracted sufficient interest. A brief review on the analogies is given. The discrepancies in the fields of initial nucleation, the upper bound of operation and the different mechanisms controlling the transport of substance and of heat in both processes are discussed.

Keywords: Bubble growth; Heat transfer; Mass transfer; Analogy

1. Introduction

Boiling at heating surfaces and gas evolution at electrodes exhibit notable analogies. Since both processes belong to strongly different fields of activity in research and industry, the analogy was not discerned for a long time. Then repeated attempts have been made to use the analogy, initially only referring to the upper operational bound [1] to be discussed below, later more generally [2–5]. This proceeding is reasonable because of numerous interrelations between the concentration field active in gas evolution and the temperature field active in boiling.

In both cases, supply of energy provides a modification of substance: In boiling, thermal energy affects a change of phases; at gas-evolving electrodes, electric energy affects an electrochemical reaction followed by the formation of a gaseous phase. In both cases, a fraction of the solid surface covered by adhering bubbles lowers the transfer area. Furthermore, growth and departure of bubbles from the wall induce microconvection controlling the heat and the mass transfer coefficient, respectively. Using the analogy is beneficial particularly for research in gas-evolving electrodes since the processes in boiling have been studied for a much longer time and are better understood than the processes in gas evolution. Using the analogy is justified because of the corresponding processes of vapour and gas formation at a wall and the resulting actions on heat and mass transfer, respectively. The charge transfer at electrodes is not more than a preceding electrochemical step to the physical process of gas formation. However, the analogy is limited, and no thorough attempts have hitherto been made to discuss this aspect. It is the object of the present paper to briefly point out the common features and to discuss the most outstanding discrepancies in both processes with the aim to contribute to a more profound understanding.

The following investigation is focussed on three particularly interesting questions:

1. Does the analogy exist with respect to the upper operational limit in both processes, or are substantially different limiting mechanisms active?
2. Does the analogy exist with respect to the initial formation of gas bubbles on electrodes and of vapour bubbles on heating surfaces? Are the critical nucleation radii the same in both processes?

* Corresponding author.
E-mail address: helmutvogt@uni.de (H. Vogt).

0017-9310/$ - see front matter © 2003 Published by Elsevier Ltd.
doi:10.1016/j.ijheatmasstransfer.2003.07.023

Nomenclature

A	electrode surface area [m^2]
c	concentration [$mol\,m^{-3}$]
d	equivalent break-off diameter [m]
D	diffusion coefficient [$m^2\,s^{-1}$]
F	Faraday constant, $F = 96487$ A s mol^{-1}
f_G	gas evolution efficiency [–]
g	acceleration due to gravity [$m\,s^{-2}$]
h	heat transfer coefficient [$W\,m^{-2}\,K^{-1}$]
Δh_v	heat of vaporization [$W\,s\,kg^{-1}$]
H	Henry coefficient [$kg\,m^{-1}\,s^{-2}$]
I	current [A]
k	mass transfer coefficient [$m\,s^{-1}$]
K	numerical factor, Eq. (1)
L	characteristic length [m]
M	molar mass [$kg\,mol^{-1}$]
n	charge number [–]
$\dot{N}$	flux of substance [$mol\,s^{-1}$]
p	pressure [$kg\,m^{-1}\,s^{-2}$]
$\dot{Q}$	heat flux [W]
R	radius of curvature [m]
R_m	universal gas constant, $R_m = 8.3143$ $kg\,m^2\,s^{-2}\,mol^{-1}\,K^{-1}$
T	temperature [K, °C]
$\dot{V}_G$	gas production rate [$m^3\,s^{-1}$]
x	molar fraction [–]
α	expansion coefficient due to concentration [$m^3\,mol^{-1}$]
γ	interfacial tension [$kg\,s^{-2}$]
ε	current efficiency [–]
η	dynamic viscosity [$kg\,m^{-1}\,s^{-1}$]
Θ	fractional shielding of the electrode surface [–]
v	stoichiometric number
ρ	density [$kg\,m^{-3}$]
Re_G	Reynolds number of gas evolution, Eq. (16)
Sc	Schmidt number, Eq. (18)
Sh	Sherwood number, Eq. (17)
St	Stanton number, Eq. (20)

Subscripts

b	gas–liquid interface
B	dissolved gas
c	critical
G	gas
L	liquid
s	saturation at plane interface
w	wall
∞	liquid bulk
0	initial nucleation

3. Does the analogy exist with respect to the mechanisms controlling the transport of substance and of heat in both processes, respectively? What are the ranges where these mechanisms are active?

2. The upper bound of nucleate gas evolution and of boiling

The upper bound of the nucleate gas or vapour evolution rate is caused by an obstruction in removal of the gaseous phase from the solid surface according to the Helmholtz instability [6,7]. The critical heat flux density, associated with the boiling crisis, may be calculated from [8,9]

$$\left(\frac{\dot{Q}}{A}\right)_c = K\Delta h_v \rho_G^{0.5}[g\gamma(\rho_L - \rho_G)]^{0.25} \tag{1}$$

with $K = 0.13 \ldots 0.16$. Inserting the properties data for *boiling* water at 100 °C gives $(\dot{Q}/A)_c = 1.2 \times 10^6$ W m^{-2} in harmony with experimental data. The corresponding critical volume flux density of vapour may be calculated with

$$\frac{\dot{V}_G}{A} = \frac{\dot{Q}}{A\rho_G \Delta h_v} \tag{2}$$

giving a critical rate $(\dot{V}_G/A)_c = 0.91$ m s^{-1}.

For *gas-evolving electrodes*, the volume flux density of gas is interrelated with the substance flux density and the current density via Faraday's law by

$$\frac{\dot{V}_G}{A} = \frac{\dot{N}}{A} f_G \frac{R_m T}{p}\left(1 - \frac{p_{H_2O}}{p}\right)^{-1} = \frac{I\varepsilon_B v_B}{AnF} f_G \frac{R_m T}{p}\left(1 - \frac{p_{H_2O}}{p}\right)^{-1}. \tag{3}$$

The term in brackets accounts for the gas–vapour mixture relevant at elevate temperatures. The parameter f_G takes account of a special feature. When bubbles are existing at an electrode, transfer of dissolved gas formed in course of an electrochemical reaction from the electrode surface occurs via two paths [10,11]. A fraction f_G is transported to the gas–liquid interface of adhering bubbles and is there transformed into the gaseous phase, Fig. 1. The complementary fraction is transported to the bulk from where it contributes to growth of freely moving bubbles, since the bulk is slightly supersaturated, or it is removed from the interelectrode gap in

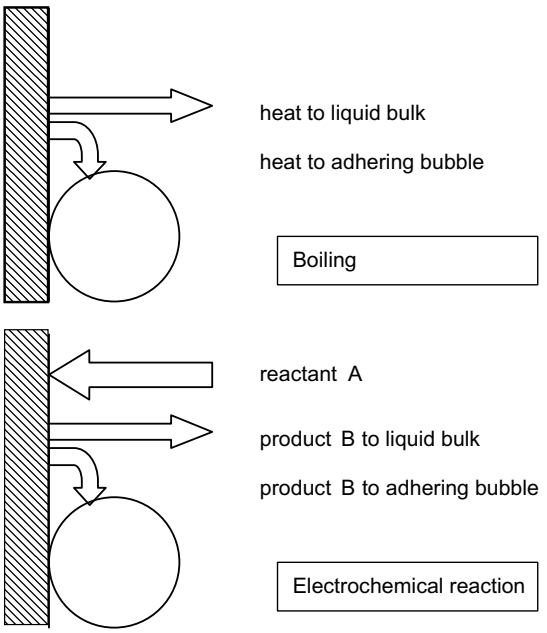

Fig. 1. Schematic comparison of the paths of heat transfer in boiling and of mass transfer at gas-evolving electrodes. In the latter case, two superimposed mass transfers are quantitatively interconnected. The directions of reactant and of product (dissolved gas) are opposite.

dissolved form with the liquid [12]. The gas evolution efficiency, f_G, depends on the bubble coverage Θ, i.e. the fraction of the total electrode area shadowed by orthogonal projection of the bubble contour to the electrode surface [13]. At large values of the current density, $f_G \approx 1$.

Experimental investigations show that the upper operational limit is reached at current densities I/A of 300–500 kA m^{-2} [14]. Although too large to be industrially relevant for most of the electrochemical processes, the values are instructive in the present context. Inserting data of hydrogen evolution at 25 °C and atmospheric pressure with $n/\nu_B = 2$ into Eq. (3) gives a rate $(\dot{V}_G/A)_c = 0.04$–0.06 m s^{-1}. The value is only about 5% of the corresponding value in boiling.

A reason of the discrepancy in both results is the fact that the surface tension γ is strongly affected by surface charges and depends on the electrode potential. Another reason must be seen in the existence of a limit, active only in electrochemical processes. In both cases, the Helmholtz criterion forms the upper limit of nucleate gas or vapour evolution, but prior to reaching this limit at electrodes a further limiting mechanism may be (and is in most cases) active which has no analogue in boiling, namely the mass transfer limitation of reactant, Fig. 1. As the bubble coverage increases with increasing current, the actual current density on the remaining active area of a gas-evolving electrode increases strongly and attains the so-called limiting current density characterized by zero concentration of reactant at the interface. Then the overpotential approaches infinity and the process breaks down. These steps are also the reason of the so-called anode effect in industrial aluminium production [15].

The analogy does further not hold if the electrode area is completely covered by the gaseous phase. In this case, electrolysis ceases. The formation of sparks at high values of the cell voltage as observed in aluminium production during the anode effect [16] is not linked with an electrochemical reaction. An analogue to film boiling does not exist at gas-evolving electrodes.

Strictly, the action of f_G should have been taken into account for boiling, too. In this process a fraction f_G of the heat is transported from the heating surface to adhering bubbles where it is transformed into the vapour phase. The complementary amount is transferred to the liquid bulk by heat conduction and convection. So Eq. (2) should be written more comprehensively

$$\frac{\dot{V}_G}{A} = \frac{\dot{N}}{A} f_G \frac{R_m T}{p} = f_G \frac{\dot{Q}}{A \Delta h_v \rho_G}. \tag{4}$$

However, a parameter corresponding to f_G is not used in heat transfer science. Reasons are discussed in Section 4.

3. Initial nucleation

We now turn to the lower bound of gas evolution. The term gas evolution continues to be understood as the formation of a gaseous phase at the wall, irrespective of whether the phase is formed of vapour in boiling or of gas or gas–vapour mixtures at gas-evolving electrodes. Experimental investigations show that there is a striking difference in the flux densities of substance $\dot{N}/A$ associated with the initial nucleation, i.e. the formation of the first gas or vapour bubble.

At *electrodes*, gas bubbles form at very small values of the current density and correspondingly small flux densities of substance of the reactant transported to the electrode and of product, i.e. dissolved gas, transported from the electrode. As an example we refer to the classical experiments of hydrogen evolution at various electrode materials conducted by Baars und Kayser [17]. At cathodes of various materials, the authors observed the first gas bubbles at a current density I/A as low as 0.004 A m^{-2}. Supposing an current efficiency $\varepsilon_B = 100\%$, this corresponds to a flux density of generated hydrogen of

$$\frac{\dot{N}}{A} = \frac{I \varepsilon_B \nu_B}{AnF} = 2 \times 10^{-8} \frac{\text{mol}}{\text{m}^2\,\text{s}}. \tag{5}$$

Similar values are found in formation of gases other than hydrogen. Following several authors, oxygen evolution starts at current densities of about 0.1 $\mathrm{A\,m^{-2}}$ [18]. The values do not differ substantially between different electrode materials. Significantly larger values can only be attained if the electrode surface is extremely smooth and free from contaminants. At ultra clean mercury cathodes, Dapkus and Sides [19] observed the incipience of bubble formation at a current density as large as 220 $\mathrm{A\,m^{-2}}$. Such a value is not characteristic of solid electrodes.

As an example of *boiling* we refer to the equally classical experiments conducted by Jakob and coworkers [20,21] with water at atmospheric pressure. Formation of the first vapour bubbles is reported to approximately coincide with the incipience of prevailing microconvective heat transfer [22] occurring at a heat flux density of about 10 $\mathrm{kW\,m^{-2}}$. The corresponding value of the flux density of substance is

$$\frac{\dot{N}}{A} = \frac{\dot{Q}}{AM\Delta h_{\mathrm{v}}} = 0.2\,\frac{\mathrm{mol}}{\mathrm{m^2\,s}}. \tag{6}$$

The striking discrepancy cannot be explained by different molar masses and deserves investigation to deliver further information on the analogy and its limitations.

3.1. Conditions of nucleation

Experience shows that solid surfaces are scattered with numerous nucleation sites which in contact with a liquid are realized as tiny gas volumes trapped in surface irregularities. At sufficient deviation from the interfacial equilibrium they become active and enable bubble growth. The equilibrium may be disturbed thermally as occurs in boiling and/or by supply of substance as occurs at electrodes. This fact permits a common treatment of both processes. Homogeneous nucleation plays a subordinate role in boiling and in gas evolution at electrodes.

The deviation of the saturation pressure at a plane interface, p_{s}, from the liquid pressure at the bubble interface, p_{b}, is given by the Thomson equation

$$p_{\mathrm{s}} - p_{\mathrm{b}} \equiv \Delta p = \frac{2\gamma}{R}\cdot\frac{\rho_{\mathrm{L}}}{\rho_{\mathrm{L}} - \rho_{\mathrm{G}}} \tag{7}$$

which is equally applicable to vapour bubbles in boiling and to gas bubbles at electrodes.

3.2. The critical nucleation radius at gas-evolving electrodes

Henry's law interrelates the pressure difference with the supersaturation of dissolved gas at the interface, written for a dissolved gas B in the liquid,

$$\Delta x_{\mathrm{B,L}} = x_{\mathrm{B,G}}\frac{\Delta p}{H}. \tag{8}$$

Introducing the concentration,

$$c_{\mathrm{B}} \equiv x_{\mathrm{B,L}}\frac{\rho_{\mathrm{L}}}{M_{\mathrm{L}}}, \tag{9}$$

results under consideration of Eq. (7) in the supersaturation at the curved interface as compared to that at a plane one,

$$\begin{aligned}\Delta c_{\mathrm{B}} &\equiv c_{\mathrm{B,b}} - c_{\mathrm{B,s}} = \Delta x_{\mathrm{B,L}}\frac{\rho_{\mathrm{L}}}{M_{\mathrm{L}}}\\ &= \frac{2\gamma\rho_{\mathrm{L}}}{RHM_{\mathrm{L}}}\left(\frac{\rho_{\mathrm{L}}}{\rho_{\mathrm{L}} - \rho_{\mathrm{G}}}\right)x_{\mathrm{B,G}},\end{aligned} \tag{10}$$

where for the common case of aqueous electrolyte solutions, the molar fraction of the species B is

$$x_{\mathrm{B,G}} = 1 - \frac{p_{\mathrm{H_2O}}}{p}. \tag{11}$$

At gas-evolving electrodes, the concentration at the gas–liquid interface, $c_{\mathrm{B,b}}$, approximately equals the concentration at the electrode prior to growth, and the bulk concentration $c_{\mathrm{B}\infty}$ approximately equals the saturation concentration, $c_{\mathrm{B}\infty} \approx c_{\mathrm{B,s}}$ [11]. Hence, the unknown supersaturation at the bubble–liquid interface Δc_{B} may be estimated from the mass transfer equation of dissolved gas transported to liquid bulk,

$$\Delta c_{\mathrm{B}} \approx c_{\mathrm{B,w}} - c_{\mathrm{B}\infty} \equiv \frac{\dot{N}_{\mathrm{B}}}{Ak}. \tag{12}$$

With Faraday's law applied to dissolved gas,

$$\frac{\dot{N}_{\mathrm{B}}}{A} = \frac{I\varepsilon_{\mathrm{B}}v_{\mathrm{B}}}{AnF}(1 - f_{\mathrm{G}}), \tag{13}$$

follows the critical radius of curvature from Eq. (10) with $f_{\mathrm{G}} \ll 1$,

$$R_{\mathrm{c}} = \frac{2\gamma A\rho_{\mathrm{L}}knF}{HI\varepsilon_{\mathrm{B}}v_{\mathrm{B}}M_{\mathrm{L}}}\frac{\rho_{\mathrm{L}}}{\rho_{\mathrm{L}} - \rho_{\mathrm{G}}}\left(1 - \frac{p_{\mathrm{H_2O}}}{p}\right). \tag{14}$$

Since the gas density is much smaller than the liquid density, $\rho_{\mathrm{G}} \ll \rho_{\mathrm{L}}$, the equation may be simplified to

$$R_{\mathrm{c}} = \frac{2\gamma A\rho_{\mathrm{L}}k(n/v_{\mathrm{B}})F}{HI\varepsilon_{\mathrm{B}}M_{\mathrm{L}}}\left(1 - \frac{p_{\mathrm{H_2O}}}{p}\right). \tag{15}$$

Eq. (15) may be rewritten in dimensionless form. Inserting dimensionless groups used in mass transfer [4]

$$\begin{aligned}Re_{\mathrm{G}} &\equiv \frac{I\varepsilon_{\mathrm{B}}R_m Td\rho_{\mathrm{L}}}{A(n/v_{\mathrm{B}})F(p - p_{\mathrm{H_2O}})\eta_{\mathrm{L}}}\\ &= \frac{I\varepsilon_{\mathrm{B}}R_m Td\rho_{\mathrm{L}}}{A(n/v_{\mathrm{B}})Fp_{\mathrm{L}}}\left(1 - \frac{p_{\mathrm{H_2O}}}{p}\right)^{-1},\end{aligned} \tag{16}$$

$$Sh \equiv \frac{kd}{D}, \tag{17}$$

$$Sc \equiv \frac{\eta_L}{\rho_L D} \tag{18}$$

gives

$$\frac{R_c H}{2\gamma} = \frac{\rho_L R_m T}{p_G M_L} \frac{Sh}{Re_G Sc} = \frac{\rho_L M_G}{\rho_G M_L} St \tag{19}$$

with the Stanton number of mass transfer

$$St \equiv \frac{Sh}{Re_G Sc}. \tag{20}$$

Every bubble nucleus with a radius of curvature $R \geqslant R_c$ is active. Since the increase in the mass transfer coefficient k (or in the Sherwood number Sh) is always smaller than the increase in the nominal current density I/A (or in the Reynolds number Re_G), the critical radius R_c decreases as I/A increases. Then the number of active nucleation sites on an electrode surface increases with the current density, as confirmed by numerous experimental investigations.

3.3. The critical nucleation radius in boiling

The interrelation between the pressure difference in Eq. (7) and the corresponding temperature difference is given by the Clapeyron–Clausius equation

$$\frac{dp}{dT} = \frac{\Delta h_v}{T_s(\rho_G^{-1} - \rho_L^{-1})} \approx \frac{p_{B,b} - p_{B,s}}{T_b - T_s}. \tag{21}$$

Inserting the fundamental heat transfer equation

$$\frac{\dot{Q}}{A} \equiv h(T_w - T_\infty) \tag{22}$$

in analogy to Eq. (12)—again with the corresponding approximation $T_b - T_s \approx T_w - T_\infty$ into Eq. (7) gives the critical radius of curvature in boiling,

$$R_c = \frac{2\gamma}{\Delta h_v \rho_G} \frac{ATh}{\dot{Q}}. \tag{23}$$

3.4. The critical radius of the first bubble in boiling and in gas evolution at electrodes

Eqs. (15) and (23) for the critical radius of curvature associated with the formation of the first gas bubble or vapour bubble allow quantitative comparison.

In *boiling*, as mentioned above, the onset of bubble formation for boiling of water at atmospheric pressure was observed by Jakob and co-workers [20,21] at a heat flux density of about $\dot{Q}/A = 10$ kW/m^2. With a heat transfer coefficient $h = 1700$ W m^{-2} K^{-1} [23] follows from Eq. (23) a critical radius $R_c = 6$ μm.

For *gas-evolving electrodes*, we refer to a current density of about $I/A = 0.1$ A m^{-2} as observed by Kabanow and Frumkin [24] at initial nucleation. With the properties of an electrolyte solution of 1 kmol m^{-3} H_2SO_4 at about 20 °C ($\gamma = 0.07$ kg s^{-2}, $H = 10^{10}$ kg m^{-1} s^{-2}, $\rho_L = 1060$ kg m^{-3}, $\eta_L = 1.23 \times 10^{-3}$ kg m^{-1} s^{-1}, $n/\nu_B = 2$) the mass transfer coefficient k of the dissolved gas for prevailing single-phase free convection was calculated from [25]

$$Sh \equiv \frac{kL}{D} = 0.72 \left[\frac{I\varepsilon_B \alpha g L^4}{A(n/\nu_B)F(\eta_L/\rho_L)^3} Sc^2 \right]^{0.2} \left[\frac{1-\Theta}{1-2/3 f_G} \right]^{0.8}. \tag{24}$$

With $\Theta \to 0$ and $f_G \to 0$ for the onset of bubble formation, the equation reduces to

$$k = 0.72 D^{0.6} \left(\frac{I\varepsilon_B \alpha g}{A(n/\nu_B)F(\eta_L/\rho_L)L} \right)^{0.2}. \tag{25}$$

Inserting an expansion coefficient due to concentration, $\alpha = 13.5 \times 10^{-6}$ m^3 mol^{-1}, estimated from [26], a diffusion coefficient $D = 3.4 \times 10^{-9}$ m^2 s^{-1} and a free flow length equal to the electrode length of presumingly $L = 0.02$ m the critical radius of the first bubble results from Eq. (15) in $R_c = 4$ μm.

The results confirm the expectation. It is seen that the critical radii of the first bubble in boiling and in gas evolution are of the same order of magnitude, although the values of the corresponding flux densities differ substantially, Fig. 2. Hence, the critical radius is not the origin of the observed discrepancy. The analogy is fulfilled in this respect, it is not with regard to the related

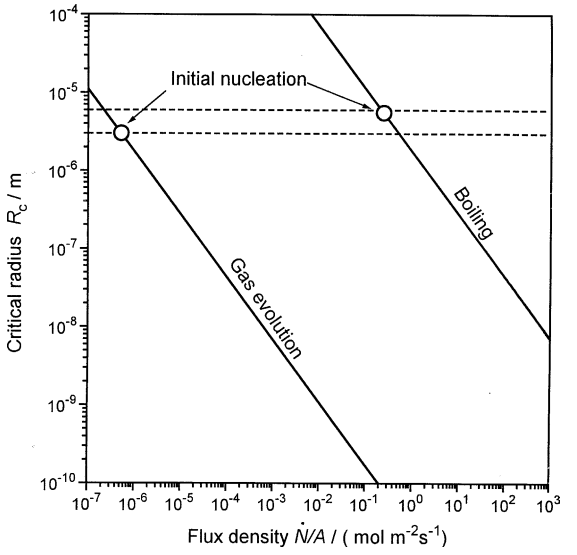

Fig. 2. Almost equal critical initial nucleation radii in gas evolution at electrodes and in boiling at strongly diverging flux densities.

flux densities. Combining Eqs. (15) and (23) with (5) and (6) and supposing equal surface tension and liquid molar mass in both systems,

$$\frac{(\dot{N}_0/A)_{\text{boiling}}}{(\dot{N}_0/A)_{\text{gas evolution}}} = \frac{T_s h H \varepsilon_B}{\Delta h_v^2 \rho_G \rho_L k} \frac{M_L}{M} \approx \frac{T_s h H \varepsilon_B}{\Delta h_v^2 \rho_G \rho_L k}, \qquad (26)$$

shows that the difference in flux rates associated with initial nucleation in boiling and in gas evolution is controlled by the physical and thermodynamic properties.

3.5. Artificial nucleation sites

It is known that nucleation in boiling can be enhanced by partial coating heating surfaces with a hydrophobic material, such as PTFE [27,28] or by direct contact of PTFE fibres with the heating surfaces [29]. By these measures artificial nucleation sites are imported, which increase the number of growing bubbles. The heat transfer is enhanced because of the increase in microconvection and in spite of the increase in bubble coverage.

The processes at gas-evolving electrodes are analogous except for the fact that the partial area covered by PTFE is insulated and inactive for charge transfer. This feature and the increased bubble coverage diminish the active electrode area. Nonetheless the overpotential was lowered after PTFE was sprayed on electrode surfaces [30,31]. The reason for this effect is that the overall population density of adhering bubbles on the surface increases, but the bubble population density on the fraction of the electrode area not covered by PTFE goes down, and this effect is the controlling one in lowering the overpotential [32].

Under certain conditions, the active electrode surface may be kept completely free of adhering bubbles by the action of artificial nucleation sites, Fig. 3. Rough fibres in contact with a smooth working electrode were found to carry enough active nucleation sites to provoke bubble formation at the fibres. Dissolved gas is transported to the bubbles growing at the fibres thus lowering the supersaturation at the electrode surface to such an extent that it remained free of bubbles. Initial nucleation at the electrode surface occurred at higher values of the current density than without PTFE fibres. It is not even necessary to attach these materials directly to the electrode surface. PTFE fibres positioned in a small distance in front of the electrode surface without contact were able to induce bubble formation. However, the effect is restricted to small values of the current density because of the difference in the controlling properties. The thickness of the diffusion layer at electrodes is only a few percent of the temperature boundary layer at heating surfaces at equal rates of the flux densities $\dot{N}/A$.

Fig. 3. Hydrogen evolution at a PTFE filament close to a stainless steel (#1.45.71) cathode surface remaining free of bubbles. The electrode surface was polished to a roughness of 0.01 μm. $I/A = 20\ \text{A m}^{-2}$, electrolyte: 1 M KOH, $T = 20$ °C.

4. Controlling transfer mechanisms

The controlling heat transfer mechanism in nucleate boiling is bubble-induced microconvection that has currently been considered the controlling mass mechanism at gas-evolving electrodes, too. However, reality is more complex.

In *boiling*, as soon as the first bubbles are formed they interfere substantially with the single-phase natural convection strongly restraining single-phase natural convection. The onset of the formation of vapour bubbles at a certain heat flux density essentially coincides with the onset of the predominance of bubble-induced microconvection. In boiling water at atmospheric pressure, the upper bound of the region of single phase heat transfer was about 10 kW m^{-2} [21].

By way of contrast, in *gas evolution* mass transfer at gas evolving electrodes in stagnant electrolyte is controlled by two effective mechanisms [33,34]. Single-phase mass transfer is not only active in the current density region without bubble formation. In an extended region after start of bubble formation, the stirring action of gas bubbles is not strong enough to modify the mass transfer mechanism. Density gradients due to concentration inside the electrode boundary layer induce a single-phase microconvection which exceeds the effect of the bubble-induced microconvection in the vicinity of adhering gas bubbles. Although bubble formation starts at current density values of about 0.1 A m^{-2}, liquid-phase natural convection continues to dominate up to about 1000 A m^{-2} [25]. The region of prevailing bubble-induced microconvection is restricted to larger current density values.

The volume flux density of evolved gas and vapour is shown in Fig. 4 for equal surface roughness represented by an initial radius of curvature $R_c = 10$ μm. Typical data of a hydrogen-evolving electrode at 25 °C and of boiling water at 100 °C were used. Line *1* for hydrogen

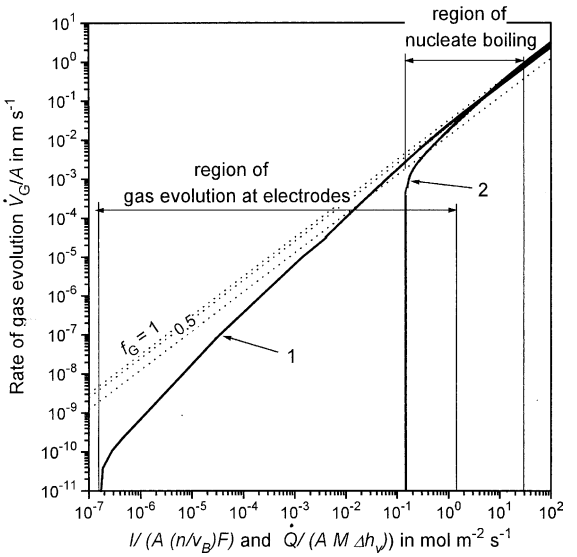

Fig. 4. Volume flux densities of evolved gas at electrodes (1—hydrogen formed at 25 °C and atmospheric pressure) and of vapour in boiling (2—water at 100 °C).

evolution at an electrode was calculated with Eq. (3), line *2* for boiling with Eq. (4). The value f_G was estimated approximately from [12]

$$f_G = 1 - (1 - \Theta)^{2.5}, \tag{27}$$

where Θ mainly depends on the current density,

$$\Theta = \left(\frac{I/A - (I/A)_0}{(I/A)_{\Theta\to 1}} \right)^{0.3}. \tag{28}$$

$(I/A)_{\Theta\to 1}$ denotes a maximum nominal current density associated with a fictitious bubble coverage extrapolated to $\Theta \to 1$. Evaluation of measured bubble coverage data suggest a value of $(I/A)_{\Theta\to 1} \approx 500$ kA m^{-2}. $(I/A)_0$ denotes the current density at initial nucleation.

Fig. 4 is informative. It is immediately seen that the region of nucleate gas evolution is much more extended than that of boiling. It is further seen that for gas-evolving electrodes a value $f_G = 0.5$ is reached at a current density about 100 000-fold the initial nucleation current density. In boiling, the same f_G value is reached at about 2-fold the initial heat flux density. Additionally the corresponding volume flux density is much larger in boiling that in gas evolution. The combined action of both effects provides an indication why the range of prevailing natural convection within the region of gas evolution is extended at gas-evolving electrodes and narrow in boiling. The finding also explains why the bubble coverage Θ and the corresponding gas evolution efficiency f_G, both quantities being very effective in gas evolution, play no role in boiling.

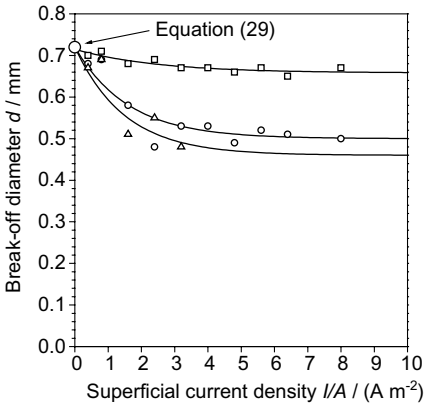

Fig. 5. Variation of the bubble break-off diameter with the current density. Evolution of hydrogen (○, □) and oxygen (△) at a nickel electrode from 1 M KOH at 20 °C.

5. Break-off diameter

A further substantial discrepancy in the analogy is the value of the bubble break-off diameter d. In boiling, it can roughly be estimated from the relation of Fritz [35], modified by Stephan [22],

$$d = 1.20\vartheta\sqrt{\frac{\gamma}{g(\rho_L - \rho_G)}}, \tag{29}$$

where ϑ is the contact angle, occasionally with corrections taking account of dynamic effects.

The equation is not simply applicable to gas-evolving electrodes where the break-off diameters are as small as about 10–50 μm. The reason is not an invalidity of Eq. (29), but the fact that increasing current density I/A varies the electrode potential affecting the wettability reflected by the contact angle. Recent own careful measurements with computer-assisted evaluation have shown that under zero current conditions equation (29) is applicable, but very small values of the current density being much lower than industrially applied values are satisfactory to lower the break-off diameter considerably, Fig. 5. As the break-off diameter is of substantial effect on microconvective mass transfer (at gas-evolving electrodes as well as in boiling), reliable knowledge of d is of great practical importance.

6. Conclusions

There are numerous analogies between nucleate boiling and gas evolution at electrodes, useful for interpretation of the processes. In both cases, the gaseous phase formed at the interface substantially interferes with the processes of heat and mass transfer. However, the analogy is limited in several aspects.

1. Using the analogy between boiling and gas evolution at electrodes it must be realized that the analogy is restricted to the transfer of substances, i.e. dissolved gas, from the electrode and the transfer of energy from the heating surface, respectively. The analogy cannot be extended to a second superimposed and quantitatively interrelated mass transfer, i.e. that of reactant transferred from the liquid bulk to the electrode. This process is not analogous to boiling with heat transfer in a single direction from the heating surface. So the analogy is restricted to the supersaturation of product in gas evolution and the superheating in boiling. It is not admissible to establish an analogy between superheating and electrode potential, as proposed by Mazza et al. [2], because the electrode potential may be essentially controlled by the interfacial concentration of *reactant*.
2. The upper bound of nucleate gas evolution at electrodes forms the upper operational limit. An analogue to film boiling does not exist at electrodes, because a gas film, although not necessarily preventing current transport, upsets electrolysis.
3. Generally, in both processes, the Helmholtz instability forms the upper operational limit of nucleate evolution of the gaseous phase. However, operation of gas-evolving electrodes is in many cases limited by a prior event, i.e. the mass transfer limitation of reactant to the electrode: When the concentration of reactant at the electrode surface approaches zero, according to the Butler–Volmer equation the electrode overpotential increases strongly and prevents further electrolysis. The analogue in boiling does not exist.
4. Electrodes and heating surfaces, provided they are of equal surface roughness, do not exhibit differences at initial nucleation with regard to the size of nucleation sites. It is irrelevant whether the nucleation is induced by supersaturation with dissolved gas or by overtemperature, respectively. However, the corresponding values of the flux densities of substance associated with the initial nucleation differ substantially. The rate for gas evolution at electrodes is larger than the corresponding rate in boiling by approximately 6 orders of magnitude, Fig. 2.
5. In boiling, the region of prevailing microconvective bubble-induced heat transfer nearly coincides with the region of bubble formation. In contrast, the microconvective mass transfer at gas-evolving electrodes is the controlling mechanism only in the upper range of gas evolution. The lower range is covered by prevailing single-phase mass transfer. The region of prevailing bubble-induced microconvection in boiling and in gas evolution at electrodes covers a range of the flux rates of only 2 orders of magnitude. Gas evolution is generally considered an effective means in enhancing mass transfer at electrodes, but the statement must be restricted to large gas flux densities.
6. The bubble break-off diameters in boiling and at gas-evolving electrodes differ strongly since in the latter case the wettability varies with the electrode potential, hence with the current density, Fig. 5.

References

[1] R. Piontelli, B. Mazza, P. Pedeferri, Comments on B.J. Welch, R.J. Snow, The repeatability of the anode effect in cryolite–alumina melts, J. Electrochem. Soc. 114 (1967) 652–654.
[2] B. Mazza, P. Pedeferri, G. Re, Hydrodynamic instabilities in electrolytic gas evolution, Electrochim. Acta 23 (1978) 87–93.
[3] K. Stephan, H. Vogt, A model for correlating mass transfer data at gas evolving electrodes, Electrochim. Acta 24 (1979) 11–18.
[4] H. Vogt, Gas evolving electrodes, in: E. Yeager, J.O'M. Bockris, B.E. Conway, S. Sarangapani (Eds.), Comprehensive Treatise of Electrochemistry, vol. 6, Plenum, New York, 1983, pp. 455–489.
[5] A.W. Bryson, D.L. Hofman, A population balance approach to the study of bubble behaviour at gas-evolving electrodes, J. Appl. Electrochem. 19 (1989) 116–119.
[6] H. von Helmholtz, Ueber atmosphaerische Bewegungen, Zur Theorie von Wind und Wellen, Sitzungsberichte der Koeniglich Preussischen Akademie der Wissenschaften Berlin 1889, pp. 761–780.
[7] L.S. Tong, Boiling Heat Transfer and Two Phase Flow, Wiley, New York, 1965, p. 138.
[8] S.S. Kutateladze, Boiling heat transfer, Int. J. Heat Mass Transfer 4 (1961) 31–45.
[9] N. Zuber, On the stability of boiling heat transfer, Trans. Am. Soc. Mech. Eng., Ser. C, J. Heat Transfer 80 (1958) 711–720.
[10] H. Vogt, The rate of gas evolution at electrodes-I, Electrochim. Acta 29 (1984) 167–173.
[11] B. Krause, H. Vogt, Effect of operational parameters on gas evolution in electrolyte bulk: possibilities of lowering interelectrode resistance, J. Appl. Electrochem. 15 (1985) 509–515.
[12] H. Vogt, The concentration overpotential of gas evolving electrodes as a multiple problem of mass transfer, J. Electrochem. Soc. 137 (1990) 1179–1184.
[13] H. Vogt, On the supersaturation of gas in the concentration boundary layer of gas evolving electrodes, Electrochim. Acta 25 (1980) 527–531.
[14] R. Piontelli, B. Mazza, P. Pedeferri, A. Tognoni, Ricerche sullo sviluppo elettrodico di gas e sugli effetti anomali che lo accompagnano, Sviluppo da soluzione acquose, Electrochim. Metall. 2 (1967) 257–287.
[15] H. Vogt, J. Thonstad, Review of the causes of anode effects, Aluminium 77 (2003) 98–102.
[16] J. Thonstad, P. Fellner, G.M. Haarberg, J. Hiveš, H. Kvande, Å. Sterten, Aluminium Electrolysis, third ed., Aluminium-Verlag, Düsseldorf, 2001.
[17] E. Baars, C. Kayser, Untersuchungen zur Überspannung des Wasserstoffs, Z. Elektrochem. 36 (1930) 428–439.
[18] K.J. Vetter, Elektrochemische Kinetik, Springer-Verlag, Berlin, 1961, p. 506.

[19] K.V. Dapkus, P.J. Sides, Nucleation of electrolytically evolved hydrogen at an ideally smooth electrode, J. Colloid Interf. Sci. 111 (1986) 133–151.
[20] M. Jakob, W. Fritz, Versuche über den Verdampfungsvorgang, Forsch. Gebiete Ingenieurwesens 2 (1931) 435–447.
[21] M. Jakob, W. Linke, Der Wärmeübergang von einer waagerechten Platte an siedendes Wasser, Forsch. Gebiete Ingenieurwesens 4 (1933) 75–81.
[22] K. Stephan, Wärmeübergang beim Kondensieren und beim Sieden, Springer, Berlin, 1988, pp. 129ff, Heat Transfer in Condensation and Boiling, Springer, Berlin, 1992.
[23] W. Fritz, Wärmeübergang an siedende Flüssigkeiten, Z. Vereines. Deutsh. Ing., Beiheft Verfahrenstech. 83 (5) (1939) 149–155.
[24] B. Kabanow, A. Frumkin, Über die Größe elektrolytisch entwickelter Gasblasen, Z. Phys. Chem., Serie A 165 (1933) 433–452, 166 (1933) 316–317.
[25] H. Vogt, The role of single-phase natural convection in mass transfer at gas evolving electrodes—II. Experimental verification, Electrochim. Acta 38 (1993) 1427–1431.
[26] H. Vogt, Prediction of the isothermal expansion coefficient of electrolyte solutions containing dissolved gases, Ber. Bunsengesellschaft Phys. Chem. 96 (1992) 158–162.
[27] R.K. Young, R.L. Hummel, Improved nucleate boiling heat transfer, Chem. Eng. Prog. 60 (7) (1964) 53–58.
[28] T. Hinrichs, E. Hennecke, H. Yasuda, The effect of plasma-deposited polymers on the nucleate boiling behaviour of copper heat transfer surface, Int. J. Heat Mass Transfer 124 (1981) 1359–1368.
[29] K.-H. Lösing, W. Leiner, Verbesserung des Wärmeübergangs beim Sieden durch Auflegen schlecht benetzbarer Keimbildner auf die Übertragungsflächen, Chem.-Ing.-Tech. 56 (1984) 943–952.
[30] O. Teschke, F. Galembeck, Effect of PTFE coverage on the performance of gas evolving electrodes, J. Electrochem. Soc. 131 (1984) 1095–1097.
[31] J. Nordlund, A. Roessler, G. Lindbergh, The influence of electrode morphology on the performance of a DMFC anode, J. Appl. Electrochem. 32 (2002) 259–265.
[32] H.-J. Heidrich, L. Müller, The effect of hydrophobic centres on the electrode surface on overvoltage in electrochemical gas evolution, Electrochim. Acta 35 (1990) 1089–1093.
[33] H. Vogt, The role of single-phase natural convection in mass transfer at gas evolving electrodes—I. Theoretical, Electrochim. Acta 38 (1993) 1421–1426.
[34] H. Vogt, Thermal effect on liquid-phase free convection at gas evolving electrodes, Int. J. Heat Mass Transfer 36 (1993) 4115–4121.
[35] W. Fritz, Berechnung des Maximnalvolumens von Dampfblasen, Phys. Z. 36 (1935) 379–384.